Journal of Environmental Radioactivity 233 (2021) 106619

Contents lists available at ScienceDirect

Journal of Environmental Radioactivity

journal homepage: http://www.elsevier.com/locate/jenvrad

Adsorption of U(VI) on the natural soil around a very low-level waste repository

Jingjing Wang [a,b], Shirong Qiang [c], Yun Wang [b], Wangsuo Wu [a], Ping Li [b,*], Haibo Qin [d,**], Qiaohui Fan [b,e]

[a] School of Nuclear Science and Technology, Lanzhou University, Lanzhou, 730000, China
[b] Northwest Institute of Eco-Environment and Resources, Chinese Academy of Sciences, Lanzhou, 730000, China
[c] Key Laboratory of Preclinical Study for New Drugs of Gansu Province, Institute of Physiology, School of Basic Medical Sciences, Lanzhou University, Lanzhou, 730000, China
[d] State Key Laboratory of Environmental Geochemistry, Institute of Geochemistry, Chinese Academy of Sciences, Guiyang, 550081, China
[e] Key Laboratory of Petroleum Resources, Gansu Province, Lanzhou, 730000, China

ARTICLE INFO

Keywords:
Uranium
Adsorption
Soil
Fe^{2+}
Organic matters

ABSTRACT

The behaviors of U(VI) in environmental media around radioactive waste disposal site are important for safety assessment of geological repositories. However, the estimation of environmental behaviors of U(VI) in natural media was insufficient. This work aimed to determine the adsorption of U(VI) on natural soil surrounding a candidate very low-level radioactive waste (VLLW) disposal site in southwest China. Results showed that the adsorption process of U(VI) on soils could be well supported by pseudo-second-order kinetic and Freundlich model. The adsorption of U(VI) was pH-dependent but temperature-independent. High ionic strength (NaCl) strongly affected the adsorption process at low pH (2.0–5.5). CO_3^{2-} remarkably inhibited the U(VI) adsorption, while the adsorption of U(VI) was promoted by PO_4^{3-} and SO_4^{2-}. Naturally occurred soil organic matters (SOMs) showed high affinity for U(VI), while the presence of additional humic acid (HA) strongly inhibited U(VI) adsorption. The occurrence of ferrous iron could result in the reduction of U(VI) at low pH values (pH $<$ 4), leading to the promotion of immobilization of U(VI). These findings would provide some guidance for the safety assessments of the VLLW disposal as well as the remediation of contaminated soil.

1. Introduction

The rapid development of nuclear power industry has caused an increasing attention to the treatment of radioactive wastes (Zhang et al., 2015). For a very low-level radioactive waste (VLLW) disposal site, shallow land geological repositories are designed as a multi-barrier system to ensure that radionuclides are not released from the site. However, over an extended period of time, the repository may be damaged by some unpredictable factors (geological activity or climate variations, such as earthquakes and landslides). Moreover, groundwater may interact with engineered barrier materials, resulting in the invalidation of barrier materials. Thus, the environmental behaviors of potentially released radionuclides in the surrounding natural ecosystems have emerged as an important concern in recent years.

As the dominant radionuclide by mass in radioactive wastes, uranium was widely concerned due to its long half-life, high solubility, and high chemotoxicity (Xie et al., 2019). In the environment, uranium typically occurs as soluble and mobile hexavalent uranium (U(VI)) species (Cao et al., 2020). The environmental behaviors of U(VI) are mainly controlled by geochemical processes such as adsorption/desorption, precipitation/diffusion, and redox reactions (Zhou et al., 2020). Adsorption plays a particularly important role in the retention and transport of U(VI) in natural systems. In recent years, the adsorption behaviors of U(VI) have been widely explored on pure minerals (muscovite, montmorillonite, calcite, attapulgite, etc.) (Niu et al., 2009, 2019; Richter et al., 2016; Troyer et al., 2016; Zhou et al., 2020; Dong et al., 2014; Kar et al., 2012) and (hydr)oxides (especially on Fe oxy (hydr)oxides) (Boland et al., 2014; Roberts et al., 2017; Sani et al.,

* Corresponding author.
** Corresponding author.
E-mail addresses: wangjj19@lzu.edu.cn (J. Wang), wuws@lzu.edu.cn (W. Wu), liping@lzb.ac.cn (P. Li), qinhaibo@eps.s.u-tokyo.ac.jp (H. Qin), fanqh@lzb.ac.cn (Q. Fan).

https://doi.org/10.1016/j.jenvrad.2021.106619
Received 28 November 2020; Received in revised form 31 March 2021; Accepted 7 April 2021
Available online 21 April 2021

2004). However, less attention has been paid to the reactions between U (VI) and natural soils. Compared with simple pure minerals and metal oxides, the adsorption behavior of cations on natural soils are generally much more complicated but more meaningful. For complicated natural soils, the adsorption behaviors of metals are usually controlled by many factors such as concentration of these ions between phases, soil components, organic matters, clay minerals, metal (hydr)oxides), and soil properties (the cation exchange capacity (CEC), grain size distribution, soil wettability, etc.) (Manojet al., 2020; Liu et al., 2020). For instance, naturally occurring organic matters in soils, such as fulvic substances (FA) and humic substances (HS), could strongly complexes with soluble U(VI), subsequently governing the adsorption/desorption process of U (VI) (Barger and Koretsky, 2011; Bordelet et al., 2018). Bednar et al. (2007) also found that the sorption of U(VI) in soils collected from Vicksburg and Yuma was strongly affected by the content of soil organic matters (SOMs). In cases for minerals containing reductive regents such as Fe^{2+}, the reduction of U(VI) may become one of the main factors controlling the environmental behaviors of U(VI) (Roberts et al., 2017). For instance, in a Fe-rich natural soil taken from a hillside spring in Iowa, the abiotic reduction and immobilization of U(VI) was observed (Lattaet al., 2012). As a consequence, a better elucidation for the behaviors of uranium in the local geological environment, especially in natural soil around disposal site is urgently needed.

To evaluate the risk assessment of potentially released U(VI), it is necessary to illustrate the behavior of U(VI) in surrounding environment. Unfortunately, to the best of our knowledge, there is a lack of systematic investigation on U(VI) interaction with natural soil around repository site, and the corresponding mechanisms remain unknown. In this study, forest soil around the VLLW repository sites in China was selected as the adsorbent to estimate the adsorption behavior of U(VI) in natural media. Various environmental factors on U(VI) adsorption were evaluated. The reaction mechanisms between U(VI) and soil were also addressed combining batch experiments and spectroscopic methods. The objectives of this study are to shed light on the pre-safety performance estimation of the VLLW repository and environmental protection.

2. Materials and methods

2.1. Materials

The stock solution of U(VI) with a concentration of 100 mg L^{-1} was prepared by dissolving $UO_2(NO_3)_2$•$6H_2O$ solids into deionized water, the pH value was adjusted to below 3.0. Soil humic acid ($C_9H_9NO_6$) was extracted from Gannan soil (Fan et al., 2009). All chemicals used in this study were of analytical grade.

Surface mineral soil (0–15 cm depth) excluding O horizon was collected from a forest near the candidate VLLW disposal site in southwest China. The type of the soil was the sandy soil. The collected samples were first passed through a 60-mesh sieve to remove big stones and vegetation roots. The samples were then dried, ground and sieved through a 200-mesh sieve.

2.2. Characterization

The mineralogical characteristics of soil were determined by Powder X-ray diffraction (XRD, D/Max-2400, Rigaku). The functional groups were measured using Fourier transform infrared spectroscopy (FT-IR, Bruker ALPHA). Element information and oxidation states of uranium were obtained using X-ray photoelectron spectroscopy (XPS, ESCALAB 250 equipped with Al Kα monochromatized source). Reference C 1s peak was corrected to 284.6 eV. X-ray fluorescence (XRF, Shimadzu XRF-1800) was used to analyze the soil elemental composition. The Visual MINTEQ 3.1 and PHREEQC were used to obtain the species distribution and saturation index, respectively.

2.3. Adsorption experiment

Kinetics estimation: 0.6 g L^{-1} soil suspension, 0.01 mol L^{-1} NaCl solution as the background electrolyte, and 0.3 mL 100 mg L^{-1} U(VI) stock solution was spiked into 10 mL polyethylene centrifuge tube. Deionized water was added to maintain the total volume to 6.0 mL. The initial pH value was then adjusted with HCl and NaOH solution to 3.3. The samples were put in a thermostatic oscillator. Thenafter, the suspensions in appropriate time intervals were filtered by 0.22 μm millipore filter and the concentration of U(VI) was measured by UV–vis spectrophotometer at wavelength ~652 nm.

Influence of pH, initial U(VI) concentration, humic acid and temperature: batch experiments were conducted under varied pH values, initial U(VI) concentrations (1–25 mg L^{-1}), HA contents (0–50 mg L^{-1}) and temperature (15–65 °C) over the pH range of 2–12 in a mixed suspension of 0.6 g L^{-1} soil and 0.01 mol L^{-1} NaCl for 24 h. The subsequent steps were the same as aforementioned kinetic estimation section. Note that the mentioned pH values in this study were the final pH at reaction equilibrium.

Influence of co-existing ions: batch experiments were conducted under varied background electrolyte concentrations (0.001–2.0 mol L^{-1} NaCl) or anions (0.01 mol L^{-1} Cl^-, CO_3^{2-}, SO_4^{2-}, and PO_4^{3-}) in the pH range of 2–12 in a mixed suspension of 0.6 g L^{-1} soil for 24 h. The subsequent steps were the same as aforementioned process.

Adsorption isotherm: batch experiments were conducted under varied U(VI) concentrations (0.2–15.0 mg L^{-1}) in a mixed suspension of 0.6 g L^{-1} soil and 0.01 mol L^{-1} NaCl. The pH values during the reaction processes were detected and adjusted for several times to maintain a final equilibrium pH values to 3.30 ± 0.05.

Desorption experiment: removing 3 mL supernatant from the adsorption isotherm samples, then spiked 3 mL 0.01 mol L^{-1} NaCl solution with the same pH into the remainder. After shaken for another 24 h, the U(VI) concentration of supernatant was measured the way same to the sorption experiment.

Adsorption of U(VI) on soils with different particles: the soils with different particle sizes were obtained using the stepwise screening method after dispersing the soil in pure water. Then the soil with particle sizes of <300 mesh, 200–300 mesh, 120–200 mesh, 60–120 mesh, 40–60 mesh were dried under 60 °C and ground to pass a 300-mesh sieve. The untreated soil and finally obtained soil were labeled as US, S1, S2, S3, S4, and S5, respectively.

Potassium dichromate oxidation method was used to determine the content of soil organic matters (SOMs) in those fractions. Detailly, certain amount of soil was heated in a mixture of potassium dichromate ($K_2Cr_2O_7$) and sulfuric acid (H_2SO_4) (10 mL, 0.4 mol L^{-1}). After digestion, oxidation and titrimetion, the organic content of soil was finally determined through titrimetion method. All the experiments were conducted in duplicate to achieve the averages, the SiO_2 powder was used for a blank titrimetion.

The adsorption efficiency (%), the amount of adsorbed U(VI) (q (mg g^{-1})), and the distribution coefficient (K_d) were obtained by the following equations:

$$Adsorption\% = \frac{C_0 - C_e}{C_0} \times 100\% \quad (1)$$

$$q_e = (C_0 - C_e) \times \frac{V}{m} \quad (2)$$

$$K_d = \frac{C_0 - C_e}{C_e} \times \frac{V}{m} \quad (3)$$

where C_0 (mg L^{-1}) and C_e (mg L^{-1}) represents the initial and equilibrium concentration of U(VI), V (L) and m (g) are the solution volume and the adsorbent mass. All the data were the average of triplicate experiments and the standard deviation was plotted as error bars.

3. Results and discussion

3.1. Characterization

The forest soil mainly consists of 51.92% SiO_2, 15.73% Al_2O_3, 11.79% Fe_2O_3, and CaO, P_2O_5, MgO, Na_2O, TiO_2, K_2O as minor components (Table S1 in the supplementary materials). The content of soil organic matter is 4.25%. The soil organic matters exhibited abundant functional groups, including carboxyl, amino, and hydroxyl (Fig. S1 in the supplementary materials), which could strongly influence the adsorption process of U(VI) on soil. The mineralogical compositions determined by XRD (Fig. S2) revealed that the major minerals in the forest soil are quartz (Qtz), albite (Ab) and clay minerals (montmorillonite (Mnt), mica (Klnt), illite (Ill), vermiculite (Vrm), chlorite (Chl)). The surface characteristics of soil was further analyzed using FT-IR spectra (Fig. S3). The broad band at 3621 and 1639 cm^{-1} could be respectively ascribed to the OH stretching vibration (from Si–OH and H_2O) and OH bending vibration (from H_2O). The bands at 917, 525 and 469 cm^{-1} could be attributed to Al–O(OH)–Al, Si–O–Al and Si–O–Si bending vibrations. The bands at 1088 and 1033 cm^{-1} was the Si–O bending vibration (Xu et al., 2008).

3.2. Batch experiments

Kinetics estimation. Adsorption kinetics was crucial for simulating the migration process of nuclide and understanding the adsorption mechanism (Xieet al., 2019; Wang and Guo, 2020). As shown in Fig. 1a, the adsorption equilibrium of U(VI) on the forest soil could be reached within 6 h and remains stable within 5 days. Three common kinetic models, pseudo-first-order, pseudo-second-order and Weber-Morris kinetic models (intra-particle size diffusion model), were fitted to discuss the adsorption process of U(VI) on forest soil. Three kinetics can be respectively represented as follows:

$$Ln(q_e - q_t) = Lnq_e - k_1 t \quad (4)$$

$$\frac{t}{q_t} = \frac{1}{k_2 q_e^2} + \frac{t}{q_e} \quad (5)$$

$$q_t = k_{id} t^{1/2} \quad (6)$$

where q_t and q_e (mg g^{-1}) are the amount of adsorbed U(VI) at time t and equilibrium, respectively; k_1 (min^{-1}), k_2^{-1} (g·(mg·min)$^{-1}$), and k_{id} (d = 1, 2, 3; mg g^{-1} $min^{-1/2}$) represent the rate constants of first-order, second-order, and intra-particle diffusion kinetics. The fitting results are displayed in Table 1. The pseudo-second-order kinetic model (Eq. (5)) fitted better for the kinetic data (R^2 = 0.999), indicating that the adsorption of U(VI) on forest soil was mainly affected by the soil content and U(VI) concentration (Ho and McKay, 2000). Subsequently, Weber-Morris model (Eq. (6)) was applied to further evaluate the mass-transfer mechanisms (Fig. 1b). The adsorption process of U(VI) on forest soil could be divided into three stages with decreasing slopes: (1) the external diffusion (film diffusion) of U(VI) through solution to the solid-liquid interface of soil particles with steep slope; (2) the gradual adsorption stage attributed to intra-particle diffusion (pore diffusion) with gentle slope (Alkanet al., 2007; Kumar et al., 2015); and (3) the

Table 1
Parameters of kinetic models for the U(VI) adsorption onto soil.

Models	Parameters	R^2
Pseudo-first-order	k_1 = 2.15 × 10^{-3} min^{-1} q_e = 0.97 mg g^{-1}	0.909
Pseudo-second-order	k_2 = 0.015 g·(mg·min)$^{-1}$ q_e = 3.97 mg g^{-1}	0.999
Weber-Morris intra-particle size diffusion	k_{i1} = 0.380 mg g^{-1} $min^{-1/2}$ k_{i2} = 0.127 mg g^{-1} $min^{-1/2}$ k_{i3} = 0.002 mg g^{-1}·$min^{-1/2}$	1.000 0.850 0.719

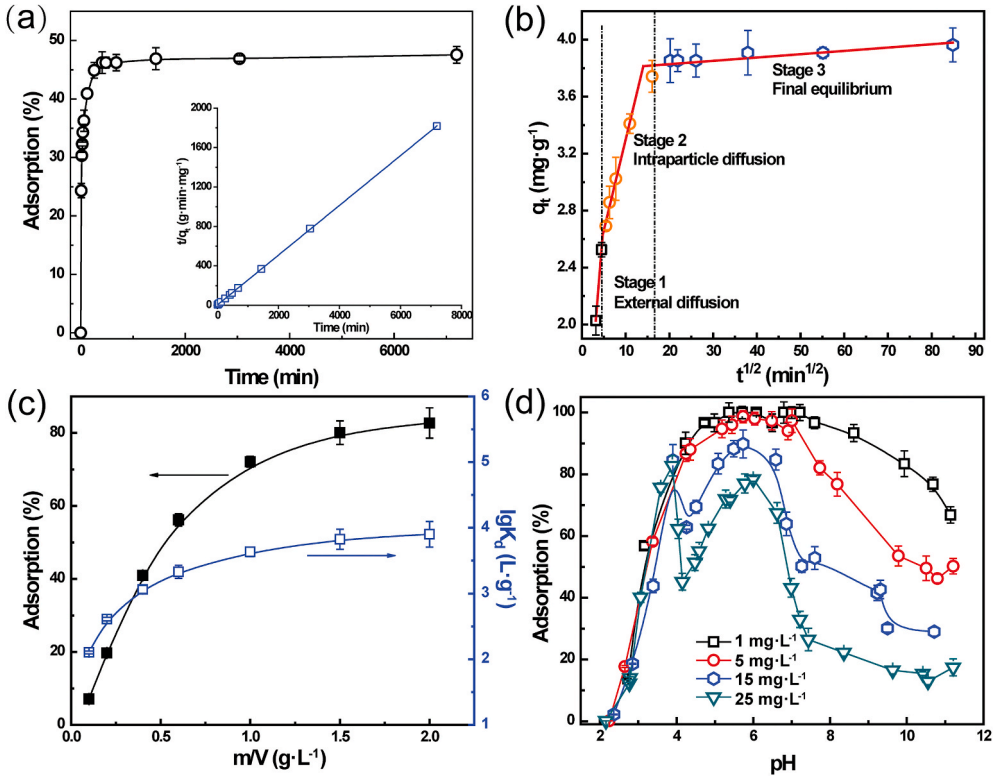

Fig. 1. The adsorption of U(VI) on soil. Effect of contact time (a); Weber-Morris kinetic model (b); Effect of solid-to-liquid ratio (c); Effect of pH and initial U(VI) concentration (d). s/l = 0.6 g L^{-1}, C(NaCl) = 0.01 mol L^{-1}, T = 25 °C.

final equilibrium stage (or reach a plateau) with a negligible slope. In addition, the diffusion rate constants for these three segments are $k_{i1} > k_{i2} > k_{i3}$ (Table 1).

Soil dose. As shown in Fig. 1c, U(VI) adsorption on soil increased with the increase in adsorbent amount. The increased adsorption capacity could be attributed by the increased number of available adsorption sites of soil (Vijayaet al., 2008; Wu et al., 2010). The relationship between the distribute efficient (K_d) and soil content (solid to liquid, *s/l*) is exhibited in Fig. 1c (blue line). In theory, the K_d value is negligibly affected by the low solid content. In this study, K_d value showed a certain increasing trend with increasing soil content. Identical results were derived by Fan et al. (2009), where the increased K_d value was caused by the locally high concentration of Ni(II) to form surface precipitate or macromolecular colloid when increasing content of attapulgite. Therefore, it is speculated in this study that there are other interactions (such as redox or complex) that promote the enrichment of U (VI) on the solid surface.

pH and the concentration of U(VI). Generally, the protonation/deprotonation of the solid surface groups and the cations species strongly depends on the solution pH, which play key roles in the adsorption of cations (Carnal and Stoll, 2011; Liu et al., 2013). Fig. 1d shows the influence of pH on the adsorption of U(VI) on forest soil with initial U(VI) concentrations range from 1.0 to 25.0 mg L^{-1}. In the acid range, the adsorption of U(VI) with low concentration increased rapidly from 0 to 100%. It could be ascribed to the decreased repulsion between UO_2^{2+} and positively charged surface when increasing pH values. Another point to note is that the adsorption of U(VI) under low pH range (2.0–4.0) in this study was significantly higher than that under similar conditions (Barger and Koretsky, 2011; Guo et al., 2009; Kumar et al., 2015; Sachs and Bernhard, 2008; Zhao et al., 2012). Interestingly, when the initial concentration of U(VI) increased to > 15.0 mg L^{-1}, two obvious peaks at pH ~3.9 and pH ~5.9 was observed. The adsorption of U(VI) showed an obvious decrease at pH > 3.9, while it was hardly affected at pH < 4.0. Typically, for the adsorption of cations on oxides or pure minerals (Erden and Donat, 2017; Wang et al., 2019; Zhou et al., 2020), the adsorption of metal ions could be inhibited over the whole pH range at higher initial concentrations. Therefore, it is considered that at pH < 4, at least one strong reaction (redox and/or strong complexation) between U(VI) and soil was involved. Under alkaline conditions, U(VI) could form anionic complexes with dissolved CO_3^{2-}, which would inhibit the adsorption of U(VI) on soil due to the electrostatic repulsion (Wang et al., 2019).

Co-existing ions. The impact of ionic strength on the adsorption of U (VI) on soil was studied by varying the concentrations of NaCl from 0.001 to 2.0 mol L^{-1}. Under acid condition (pH < 4) (Fig. 2a and b), the increase of NaCl concentration up to 1.0 mol L^{-1} led to a weakly decrease in U(VI) adsorption, which could be attributed to the slight competitive adsorption of Na^+ for active sites. Interestingly, an obvious increase in the adsorption of U(VI) in the presence of 2.0 mol L^{-1} NaCl was observed, and it was inconsistent with most sorption systems (Sheng et al., 2015; Sihn et al., 2016; Tan et al., 2018). It was known that soil properties including pH and ionic strength of the water phase directly determine organic matter solubility (Chantigny, 2003). Therefore, in the acid condition (pH ~3.3), some SOMs component (such as fulvic acid) could be easily dissolved into solution. When further increasing NaCl concentration to 2.0 mol L^{-1}, the adsorption of soluble SOMs on soil was

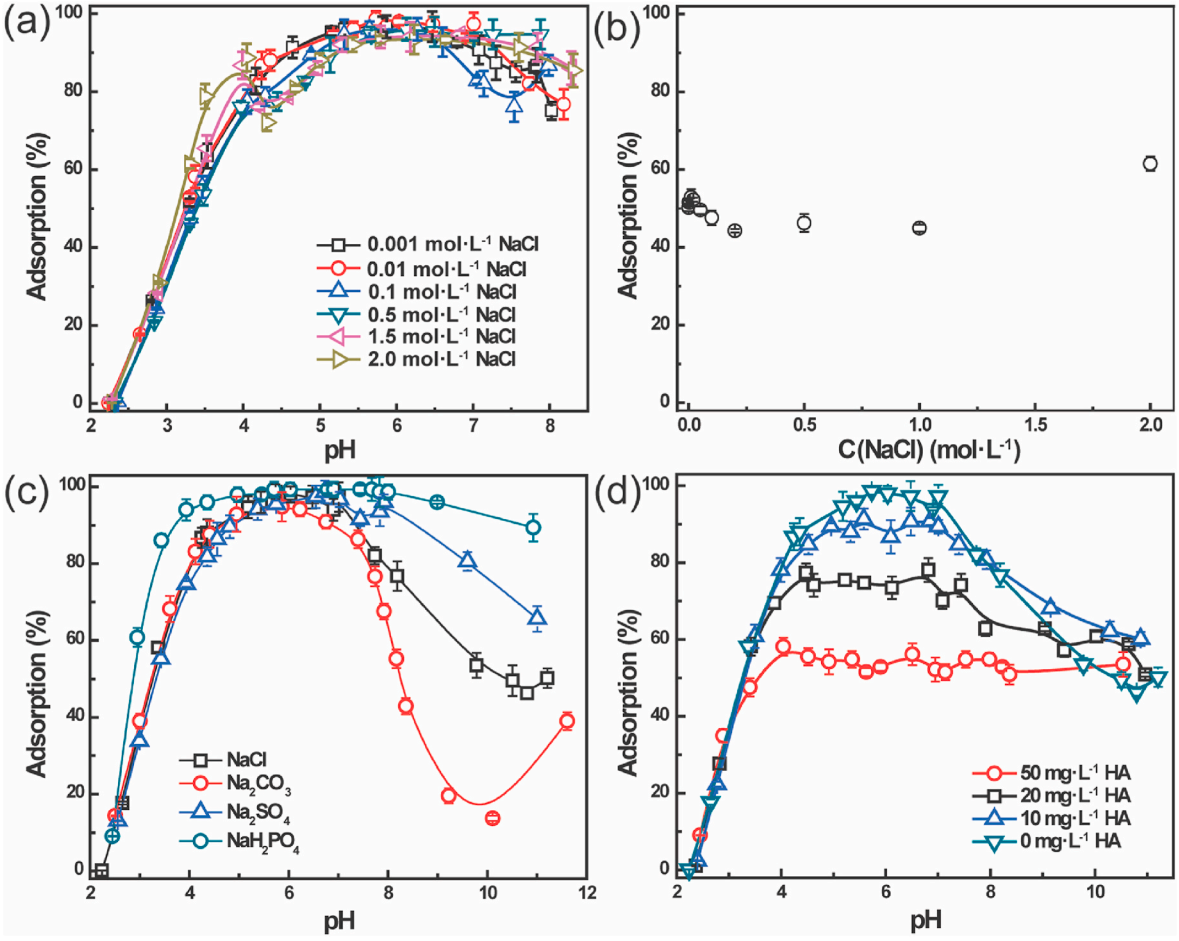

Fig. 2. Influence of environmental factors on the adsorption of U(VI) on soil. Effect of ionic strength under different pH values (a) and under pH ~3.3 (b); Effect of coexisting anions (c); Effect of HA (d). $C(UO_2^{2+})$ = 5 mg L^{-1}, *s/l* = 0.6 g L^{-1}, T = 25 °C.

enhanced, resulting in the increased U(VI) adsorption. Similar results was reported by Li et al. (2011) that in the presence of humic substance, the sorption of Eu(III) on iron oxides was enhanced when Na^+ concentration was above 0.05 mol L^{-1}. While in the absence of HA, the sorption ability gradually decreased with increasing ionic strength from 0 to 0.2 mol L^{-1}.

Given the complex environment conditions, anions were also ubiquitous in the environment that can form strong complexes with target metal ions and highly affect the physical and chemical behavior of metal ions (Zhang et al., 2018). Fig. 2c shows the effect of common electrolyte anions (Cl^-, CO_3^{2-}, SO_4^{2-}, PO_4^{3-}) on the adsorption of U(VI) on soil. The presence of CO_3^{2-} decreased U(VI) adsorption under alkaline condition. Visual Minteq program was further used to predict the concentrations and distributions of U(VI) species. As shown in Fig. S4d, $UO_2(CO_3)_2^{2-}$ and $UO_2(CO_3)_3^{4-}$ would form under alkaline condition in the presence of CO_3^{2-}, which are difficult to be adsorbed to the negatively charged surface of soil due to the repulsion. At whole pH range, the uptake enhancement in the presence of PO_4^{3-} can be attributed to the strong surface complexation between phosphate and UO_2^{2+} (Fig. S4). Similar observations have been previously reported that the adsorption of U(VI) on goethite was promoted in the presence of phosphate by the formation of ternary "adsorbent-anion-metal ion" complex (Cheng et al., 2004). The presence of SO_4^{2-} has a negligible influence on U(VI) adsorption when pH < 7. It may be due to the weak affinity between SO_4^{2-} and soil (Van Der Weijden et al., 1997). Moreover, although complexes of SO_4^{2-} with U(VI) (e.g. UO_2SO_4 and $UO_2(SO_4)_2^{2-}$) were formed (as shown in Fig. S4b), due to the occurrence of the strong interactions of U(VI) with the soil surface, the formed complexes may be insufficient to bring any change. While at pH > 7, the presence of SO_4^{2-} increased U(VI) adsorption (Fig. 2c). It is known that in the presence of SO_4^{2-}, the salting-out effect of CO_2 is much stronger than that in Cl^- solution (Yan and Chen, 2010). Therefore, the CO_2 solubility to form CO_3^{2-} was decreased in the presence of SO_4^{2-}, thus to inhibit the formation of U(VI)-carbonate complex and improved the adsorption of U(VI).

Influence of humic substance. The adsorption and migration of U(VI) could be strongly influenced by naturally occurring organic matters that widely distributed in the environment (Dubeet al., 2001; Chen et al., 2007). Given the large specific surface area, complex structure and various functional groups (Zhang et al., 2020), organic matters could affect the environmental behavior of metal ions by: (1) redox with metal ion by reduction groups; (2) change the surface morphology and exposed active sites of sorbents through surface interaction; (3) change the chemical speciation of metal ions due to the strong complexing ability. The pH-dependence of U(VI) adsorption on soil in the absence and presence of humic acid (HA) is shown in Fig. 2d. The presence of HA has almost no effect on U(VI) adsorption at low pH value (pH 2.0–3.5), while inhibiting U(VI) adsorption at pH > 3.5. Generally, the presence of HA is reported to promote the adsorption of metal ions at low pH due to the formation of ternary metal–HA–sorbents (Fan et al., 2014). Therefore, the HA-independence at low pH in this study supports the previous speculation that U(VI) adsorbed on soil dominantly via some strong interactions, which were hardly disturbed by other factors. As the pH value increases, most HA molecules remaining in solution tend to form soluble U-HA complexes with U(VI), inhibiting the adsorption of U(VI) (Wang et al., 2019; Zhao et al., 2012).

Effect of temperature on U(VI) adsorption. Temperature is one of the main factors affecting the adsorption process of metal ions (Al-anber et al., 2011; Soliman et al., 2020; Ten Hulscher et al., 1996; Uddin et al., 2017; Fan et al., 2012; Tertre et al., 2006; Yang et al., 2010). In most chemical adsorption systems, higher temperature will promote the adsorption of metal ions. Dynamically, increasing the temperature could increase the diffusion rate of adsorbent particles across the solid–liquid interface and in the internal pores (Wang et al., 2005). It may be related to accelerating some slower adsorption steps or blocking some processes such as molecular aggregation, ion pairing and complex formation (Johnson, 1990). Thermodynamically, higher temperature can boost the hydrolysis of metal ion and reduce the electrostatic repulsion between adsorbent and adsorbate, making the adsorption reactions easier to happen (Alkanet al., 2007; Sharma and Tomar, 2011). In this study, the effect of temperature (15, 25, 45, and 65 °C) on the adsorption of U(VI) on soil was conducted by varying pH values from ~2 to ~12 (Fig. 3a). Contrary to what is usually observed, temperature had no significant impact on the U(VI) adsorption. The result further confirmed the above deduction that the adsorption of U(VI) under this condition was controlled by some interactions which weakly depended on temperature.

Adsorption isotherm. Adsorption isotherm can help describe the distribution information of metal ions between the liquid phase and the solid phase (Foo and Hameed, 2010). As is illustrated in Fig. 3b, the adsorption of U(VI) on soil gradually increased at 0.2–12.0 mg L^{-1} U(VI) concentrations, then suddenly increased when U(VI) concentration reached to 15 mg L^{-1}. Generally, the sharp increase in adsorption is mainly attributed to the hydrolysis of U(VI) with high concentration to form precipitates (Bai et al., 2015). But in this study, the concentration of U(VI) and pH value is too low (~3.3) for U(VI) to form surface precipitates (as supported by the negative saturation index from Fig. S5). As discussed above, the sharp increase may be relevant to other strong interaction, which controlled the adsorption process at low pH values.

In order to better understand the interaction mechanisms between uranium and soil, four thermodynamic models (Langmuir, Freundlich, Langmuir-Freundlich and Dubinin–Radushkevich (D–R) models) were adopted to fit the experimental data (excluding the sudden rise data). The equations are expressed as follows:

$$\text{Langmuir model: } q_e = \frac{q_{\max} K_L C_e}{1 + K_L C_e} \tag{7}$$

$$\text{Freundlich model: } q_e = K_f C_e^{\frac{1}{n}} \tag{8}$$

$$\text{Langmuir} - \text{Freundlich model: } q_e = \frac{q_{\max} b C_e^{\frac{1}{n}}}{1 + b C_e^{\frac{1}{n}}} \tag{9}$$

$$\text{D} - \text{R model: } q_e = q_{\max} \exp(-K\varepsilon^2) \tag{10}$$

$$\varepsilon = -RT\lg(1 + 1/C_e) \tag{11}$$

where q_{max} (mg g^{-1}), the adsorption capacity at equilibrium; K_L (L mg^{-1}), the Langmuir constant; K_F and n, the Freundlich constants; b, Langmuir-Freundlich model; K, the D-R constant; ε, the Polanyi potential; T (K), the temperature; R, the gas constant (8.31 J mol^{-1} K^{-1}). According to the fitting results in Fig. 3b and Table 2, U(VI) adsorption on soil was in accordance with the Freundlich model, indicating that complex interaction mechanisms are possibly involved in the adsorption process.

Fig. 4a exhibited the adsorption and desorption isotherms of U(VI) on soil. The desorption isotherm deviated obviously from adsorption isotherm (sorption-desorption hysteresis), especially at high U(VI) concentration, illustrating the irreversible process. The irreversible tendency was possibly due to the strong interaction that is not easily desorbed from soil surface. It has been reported that strong complexation between organic matters and metal ions could promote the sorption irreversibly (Li et al., 2016). U(VI) sorption to Fe/Mn oxides was also confirmed to be irreversible and is not affected by high salinity (Rout et al., 2015). In addition, some processes involving U(VI) reduction or the formation of (surface) U(IV) precipitation would also affect the sorption reversibility (Missanaet al., 2004).

3.3. Mechanisms for U(VI) interaction with soil

As discussed above, some strong interactions might involve in the adsorption process between U(VI) and soil. To elucidate the reaction mechanisms between U(VI) and the forest soil, U(VI) adsorption on soil

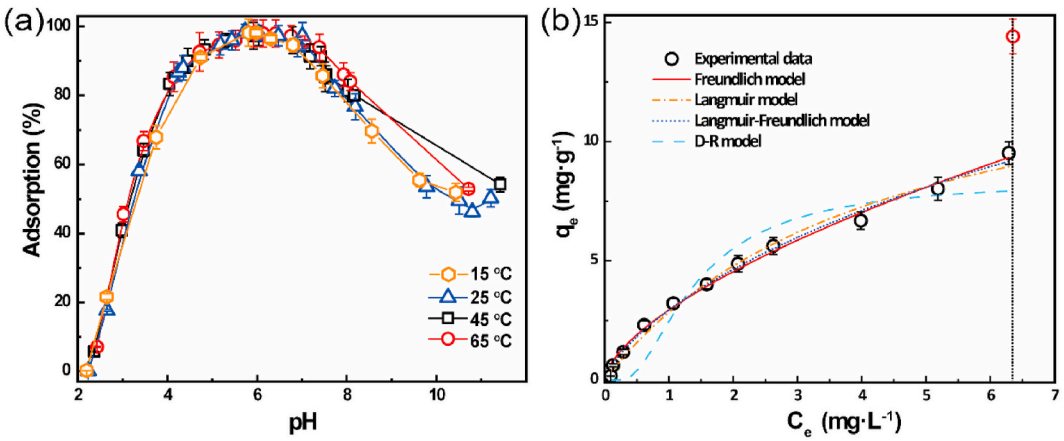

Fig. 3. Thermodynamics estimation on the adsorption of U(VI) on soil. Effect of temperature (a); The adsorption isotherm (b). s/l = 0.6 g L^{-1}, C(NaCl) = 0.01 mol L^{-1}.

Table 2
Parameters of isotherm models for the U(VI) adsorption onto soil.

Models	Parameters	AIC
Langmuir	K_L = 0.232 L mg^{-1} q_{max} = 15.08 mg g^{-1}	0.829
Freundlich	K_f = 2.939 mg^{1-n} g^{-1} L^n n = 1.591	0.420
Langmuir- Freundlich	q_{max} = 35.389 mg g^{-1} b = 0.091 L mg^{-1} n = 1.350	0.490
D-R	q_{max} = 8.383 mg g^{-1} K = 4.153 × 10^{-7} mol^2 J^{-2}	4.810

Note: AIC = 2k-2ln(L); L = -(n/2) × ln(2 × pi)-(n/2) × ln(sse/n)-n/2.

particles with different size was conducted. As shown in Fig. 4b, the adsorption of U(VI) was obviously influenced by the soil particles with different size. At acid condition, U(VI) adsorption on S1, S2 and S3 is almost the same as that on untreated soil (US), and was inhibited on S4 and S5. When pH > 7, U(VI) adsorption on soil followed the sequence of S5 < S4 < S1 ≈ US < S2 ≈ S3. It is worth to note that the formation of U (VI)-carbonate complexes would lead to the low adsorption of U(VI) on most minerals at alkaline conditions (Li et al., 2014; Tournassat et al., 2018). In this study, the high adsorption of U(VI) at high pH values was expected to derive from the occurrence of SOMs. As shown in Fig. 4c, the measured SOMs content followed the sequence of S3 > S2 > S1 > S4 > S5, which have a positive correlation with U(VI) adsorption (R = 0.982, P < 0.05). The reaction between U(VI) and soil surface at alkaline condition strongly relied on the content of SOMs in soil, high SOM concentration could increase U(VI) adsorption by forming strong complex with U(VI). This also supports the above result that high concentration of background electrolyte would enhance the adsorption of U(VI) due to the re-adsorption of soluble SOMs at acid condition. It should be noted that the adsorption percentage of U(VI) onto S4 and S5 increased again at pH > 9.0 (Fig. 4b). Similar adsorption trends were reported by Fan et al. (2014) and Kenney et al. (2017). The SOMs content for S4 (2.46%) and S5 (0.74%) was too low and should not be the dominate factor controlling the adsorption of U(VI) in alkaline conditions. The increase in U(VI) adsorption again above pH 9.0 onto S4 and S5 may be attributed to the formation of uranate-type minerals (e.g. $Na_2U_2O_7$) on the surface of soils. However, under acid condition, US (4.25%) and S1 (4.04%) with relatively low SOMs content showed similar adsorption trends with that of S2 (5.13%) and S3 (6.59%). This indicates that the adsorption ability was not directly related to SOMs content at low pH values. Under acidic conditions, U(VI) typically have strong affinity to various minerals in soil, and SOMs should not be the only factor controlling the adsorption of U(VI) (Shi et al., 2019).

As mentioned above, natural reductive ions may also strongly affect the environmental behaviors of U(VI) by reducing U(VI) to immobile U (IV). The Fe 2p$_{3/2}$ spectrum of soil depicted in Fig. 5a can be fitted into four peaks centered at 709.6, 711.5, 713.0 and 715.7 eV, which was respectively assigned to Fe(II)–O, Fe(III)–O, Fe(III)–F, and Fe(II)–O satellite peak (He et al., 2017; Yang et al., 2018). The results directly indicate that a certain amount of Fe(II) exists in the soil and may be involved in the redox reactions. The high-resolution U 4f spectra of samples after reaction with soil under pH ~2.5 was illustrated in Fig. 5b. Compared with standard U(VI) refer, with binding energy (B.E.) of 382.4 and 393.3 eV, external peaks at 380.6 and 391.6 eV could be ascribed to U(IV) phase (Wang et al., 2019, 2020; Li et al., 2019). The calculated atom% of U(IV) and U(VI) was 65.8% and 34.2%, respectively, indicating the partial reduction of U(VI) occurred at the soil-U interface at low pH value. The strong reductive immobilization was responsible for enhanced U(VI) adsorption at low pH values. In contrast, at a higher pH value (~4.7), U(VI) reduction disappeared (Fig. 5b), which may be due to the negligible dissolution of Fe^{2+} from soil.

To verify the role of SOMs and Fe^{2+} on U(VI) adsorption, soil was further treated under high temperatures (400 and 600 °C) to remove such reductive iron and SOMs components. As illustrated in Fig. 4d, the removal of Fe^{2+} and SOMs caused an obvious decrease in the U(VI) adsorption compared to the raw soil. After removing Fe(II) and SOMs, the adsorption of U(VI) was mainly controlled by the interaction on the surface soil minerals. The results further proved the promoted effect of SOMs and reductive iron on U(VI) immobilization in natural soil.

4. Conclusions

Adsorption behavior and interface interaction mechanisms of U(VI) on natural soil near VLLW disposal site were investigated comprehensively by batch experiments and spectroscopic techniques. The adsorption process of U(VI) on soil fitted the pseudo-second-order kinetic and Freundlich model well. The occurrence of SOMs in soil caused a strong complexation with U(VI). At relatively low pH values (<4.0), U(VI) could be reductively immobilized by Fe(II) in soil. Both strong complexation and reduction play a major contribution for promoting the adsorption of U(VI) on natural soil, and made the adsorption negligibly affected by temperature and ionic strength. While at particularly high Na^+ concentration, the adsorption was enhanced at low pH due to the re-adsorbed soluble organic matters on soil surface. It is expected to provide some performance assessments of geological disposal sites containing very low-level nuclear wastes.

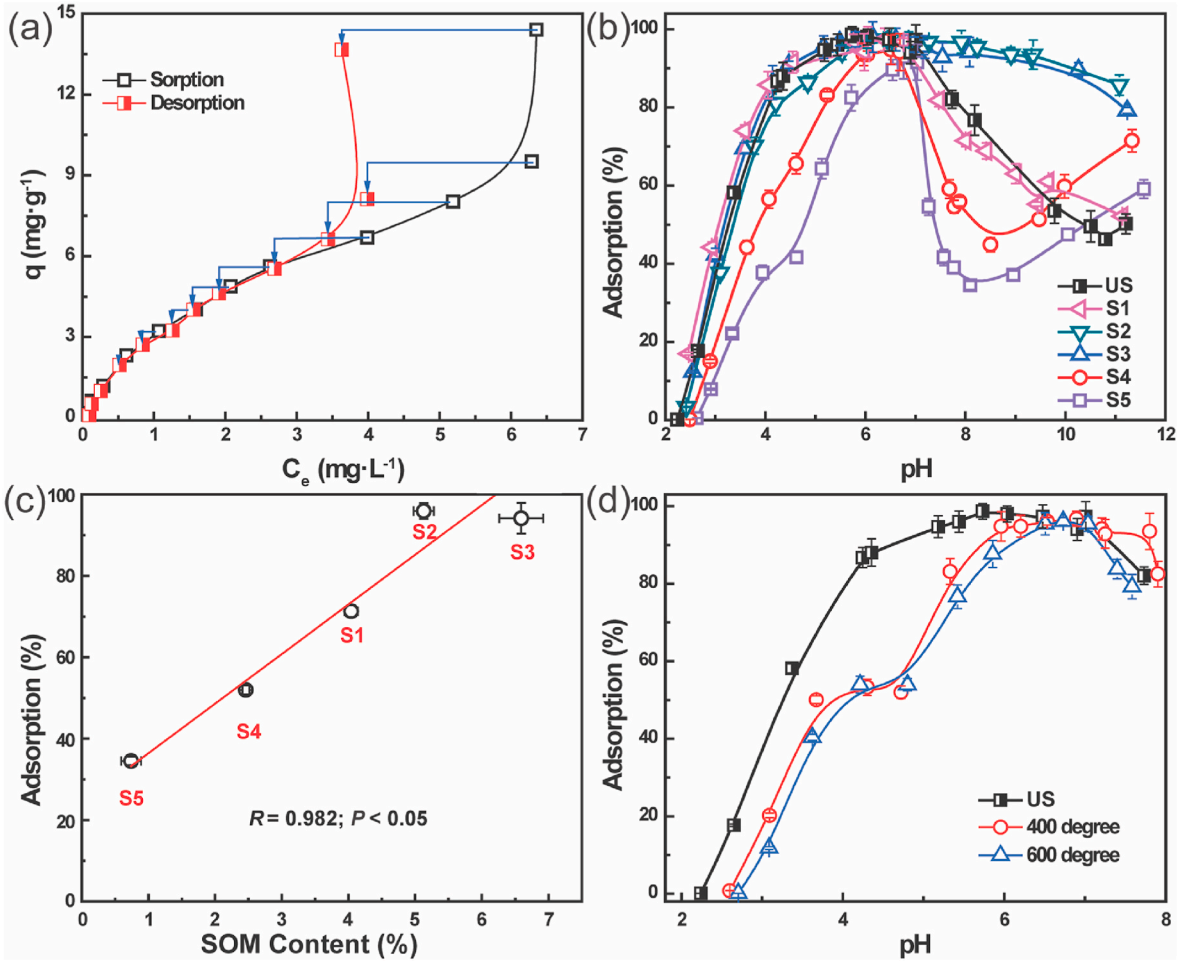

Fig. 4. The desorption of U(VI) (a); The adsorption of U(VI) on soil with different particle size (b); The correlation between U(VI) adsorption and SOMs content at pH ~8.0 (c); The adsorption of U(VI) on soil treated under different temperatures (d). $C(UO_2^{2+})$ = 5 mg L^{-1}, s/l = 0.6 g L^{-1}, C(NaCl) = 0.01 mol L^{-1}, T = 25 °C.

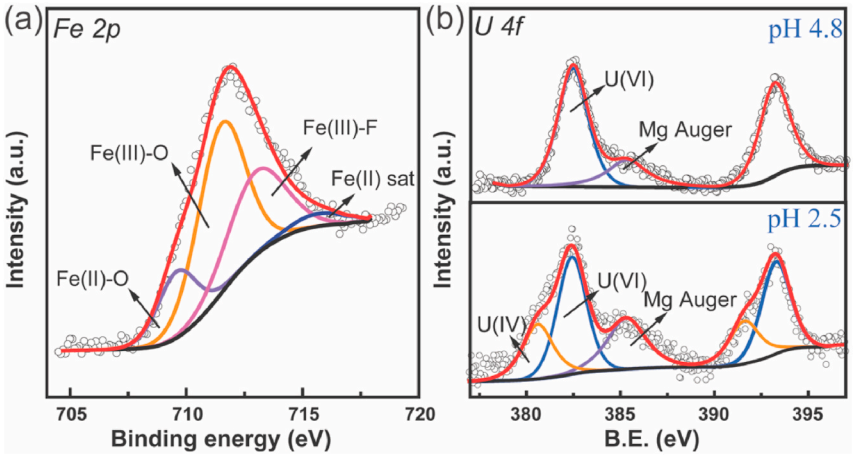

Fig. 5. Fe 2p (a) and U 4f (b) XPS spectra of U(VI) adsorbed soil. $C(UO_2^{2+})$ = 25 mg L^{-1}, s/l = 0.6 g L^{-1}, T = 25 °C, C(NaCl) = 0.01 mol L^{-1}.

Declaration of competing interest

The authors declare that they have no known competing financial interests or personal relationships that could have appeared to influence the work reported in this paper.

Acknowledgement

Financial supports from National Natural Science Foundation of China (21876172), the "Youth Innovation Promotion Association CAS", Gansu Talent and Intelligence Center for Remediation of Closed and Old Deposits, and the Key Laboratory Project of Gansu Province (1309RTSA041) are acknowledged.

Appendix A. Supplementary data

Supplementary data to this article can be found online at https://doi.org/10.1016/j.jenvrad.2021.106619.

References

Al-anber, M.A., 2011. Thermodynamics approach in the adsorption of heavy metals. Thermodyn –Interact Stud – Solids, Liq Gases 737–764. https://doi.org/10.5772/21326.

Alkan, M., Demirbaş, Ö., Doğan, M., 2007. Adsorption kinetics and thermodynamics of an anionic dye onto sepiolite. Microporous Mesoporous Mater. 101, 388–396. https://doi.org/10.1016/j.micromeso.2006.12.007.

Bai, Z.Q., Yuan, L.Y., Zhu, L., Liu, Z.R., Chu, S.Q., Zheng, L.R., Zhang, J., Chai, Z.F., Shi, W.Q., 2015. Introduction of amino groups into acid-resistant MOFs for enhanced U(vi) sorption. J. Mater. Chem. A 3, 525–534. https://doi.org/10.1039/c4ta04878d.

Barger, M., Koretsky, C.M., 2011. The influence of citric acid, EDTA, and fulvic acid on U (VI) sorption onto kaolinite. Appl. Geochem. 26, S158–S161. https://doi.org/10.1016/j.apgeochem.2011.03.092.

Bednar, A.J., Medina, V.F., Ulmer-Scholle, D.S., Frey, B.A., Johnson, B.L., Brostoff, W.N., Larson, S.L., 2007. Effects of organic matter on the distribution of uranium in soil and plant matrices. Chemosphere 70, 237–247. https://doi.org/10.1016/j.chemosphere.2007.06.032.

Boland, D.D., Collins, R.N., Glover, C.J., Payne, T.E., Waite, T.D., 2014. Reduction of U (VI) by Fe(II) during the Fe(II)-accelerated transformation of ferrihydrite. Environ. Sci. Technol. 48, 9086–9093. https://doi.org/10.1021/es501750z.

Bordelet, G., Beaucaire, C., Phrommavanh, V., Descostes, M., 2018. Chemical reactivity of natural peat towards U and Ra. Chemosphere 202, 651–660. https://doi.org/10.1016/j.chemosphere.2018.03.140.

Cao, X.Y., Zheng, L.G., Hou, D.Y., O'Connor, D., Hu, L.T., Wu, J., 2020. Modeling the risk of U(VI) migration through an engineered barrier system at a proposed Chinese high-level radioactive waste repository. Sci. Total Environ. 707, 135472. https://doi.org/10.1016/j.scitotenv.2019.135472.

Carnal, F., Stoll, S., 2011. Adsorption of weak polyelectrolytes on charged nanoparticles. Impact of salt valency, pH, and nanoparticle charge density. Monte carlo simulations. J. Phys. Chem. B 115 (42), 12007–12018.

Chantigny, M.H., 2003. Dissolved and water-extractable organic matter in soils: a review on the influence of land use and management practices. Geoderma 113, 357–380. https://doi.org/10.1016/S0016-7061(02)00370-1.

Chen, C.L., Xu, D., Tan, X.L., Wang, X.K., 2007. Sorption behavior of Co(II) on γ-Al_2O_3 in the presence of humic acid. J. Radioanal. Nucl. Chem. 273, 227–233. https://doi.org/10.1007/s10967-007-0741-9.

Cheng, T., Barnett, M.O., Roden, E.E., Zhuang, J., 2004. Effects of phosphate on uranium (VI) adsorption to goethite-coated sand. Environ. Sci. Technol. 38, 6059–6065. https://doi.org/10.1021/es040388o.

Dong, W.M., Wan, J.M., 2014. Additive surface complexation modeling of uranium(VI) adsorption onto quartz-sand dominated sediments. Environ. Sci. Technol. 48, 6569–6577. https://doi.org/10.1021/es501782g.

Dube, A., Zbytniewski, R., Kowalkowski, T., Cukrowska, E., Buszewski, B., 2001. Adsorption and migration of heavy metals in soil. Pol. J. Environ. Stud. 10, 1–10.

Erden, K.E., Donat, R., 2017. Removal of thorium(IV) from aqueous solutions by natural sepiolite. Radiochim. Acta 105, 187–196. https://doi.org/10.1515/ract-2016-2667.

Fan, Q.H., Hao, L.M., Wang, C.L., Zheng, Z., Liu, C.L., Wu, W.S., 2014. The adsorption behavior of U(VI) on granite. Environ. Sci.: Proc. Imp. 16, 534–541. https://doi.org/10.1039/c3em00324h.

Fan, Q.H., Xu, J.Z., Niu, Z.W., Li, P., Wu, W.S., 2012. Investigation of Cs(I) uptake on Beishan soil combined batch and EDS techniques. Appl. Radiat. Isot. 70, 13–19. https://doi.org/10.1016/j.apradiso.2011.07.004.

Fan, Q.H., Shao, D.D., Lu, Y., Wu, W.S., Wang, X.K., 2009. Effect of pH, ionic strength, temperature and humic substances on the sorption of Ni(II) to Na-attapulgite. Chem. Eng. J. 150, 188–195. https://doi.org/10.1016/j.cej.2008.12.024.

Foo, K.Y., Hameed, B.H., 2010. Insights into the modeling of adsorption isotherm systems. Chem. Eng. J. 156, 2–10. https://doi.org/10.1016/j.cej.2009.09.013.

Guo, Z.J., Li, Y., Wu, W.S., 2009. Sorption of U(VI) on goethite: effects of pH, ionic strength, phosphate, carbonate and fulvic acid. Appl. Radiat. Isot. 67, 996–1000. https://doi.org/10.1016/j.apradiso.2009.02.001.

He, J.G., Ma, B., Kang, M.L., Wang, C.L., Nie, Z., Liu, C.L., 2017. Migration of ^{75}Se(IV) in crushed Beishan granite: effects of the iron content. J. Hazard Mater. 324, 564–572. https://doi.org/10.1016/j.jhazmat.2016.11.027.

Ho, Y.S., McKay, G., 2000. The kinetics of sorption of divalent metal ions onto sphagnum moss peat. Water Res. 34, 735–742. https://doi.org/10.1016/S0043-1354(99)00232-8.

Johnson, B.B., 1990. Effect of pH, temperature, and concentration on the adsorption of cadmium on goethite. Environ. Sci. Technol. 24, 112–118. https://doi.org/10.1021/es00071a014.

Kar, A.S., Kumar, S., Tomar, B.S., 2012. U(VI) sorption by silica: effect of complexing anions. Colloids Surf., A 395, 240–247. https://doi.org/10.1016/j.colsurfa.2011.12.038.

Kenney, J.P.L., Kirby, M.E., Cuadros, J., Weiss, D.J., 2017. A conceptual model to predict uranium removal from aqueous solutions in water–rock systems associated with low- and intermediate-level radioactive waste disposal. RSC Adv. 7 https://doi.org/10.1039/C6RA26773D, 7876–788.

Kumar, A., Rout, S., Mishra, M.K., Karpe, R., Ravi, P.M., Tripathi, R.M., 2015. Impact of particle size, temperature and humic acid on sorption of uranium in agricultural soils of Punjab. SpringerPlus 4. https://doi.org/10.1186/s40064-015-1051-2.

Latta, D.E., Boyanov, M.I., Kemner, K.M., O'Loughlin, E.J., Scherer, M.M., 2012. Abiotic reduction of uranium by Fe(II) in soil. Appl. Geochem. 27, 1512–1524. https://doi.org/10.1016/j.apgeochem.2012.03.003.

Li, P., Fan, Q.H., Pan, D.Q., Liu, S.P., Wu, W.S., 2011. Effects of pH, ionic strength, temperature, and humic acid on Eu(III) sorption onto iron oxides. J. Radioanal. Nucl. Chem. 289, 757–764. https://doi.org/10.1007/s10967-011-1153-4.

Li, P., Yin, Z.X., Lin, J.F., Jin, Q., Du, Y.F., Fan, Q.H., Wu, W.S., 2014. The immobilization of U(VI) on iron oxyhydroxides under various physicochemical conditions. Environ. Sci.: Proc. Imp. 16, 2278–2287. https://doi.org/10.1039/c4em00301b.

Li, P., Wang, J.J., Wang, Y., Liang, J.J., He, B.H., Pan, D.Q., Fan, Q.H., 2019. Photoconversion of U(VI) by TiO_2: an efficient strategy for seawater uranium extraction. Chem. Eng. J. 365, 231–241. https://doi.org/10.1016/j.cej.2019.02.013.

Li, S.C., Wang, X.L., Huang, Z.Y., Du, L., Tan, Z.Y., Fu, Y.B., Wang, X.L., 2016. Sorption and desorption of uranium(VI) on GMZ bentonite: effect of pH, ionic strength, foreign ions and humic substances. J. Radioanal. Nucl. Chem. 308, 877–886. https://doi.org/10.1007/s10967-015-4513-7.

Liu, J.F., Wang, Z.L., Hu, F.N., Xu, C.Y., Ma, R.T., Zhao, S.W., 2020. Soil organic matter and silt contents determine soil particle surface electrochemical properties across a long-term natural restoration grassland. Catena 190, 104526. https://doi.org/10.1016/j.catena.2020.104526.

Liu, Y.H., Li, Q., Cao, X.H., Wang, Y.Q., Jiang, X.H., Li, M., Hua, M., Zhang, Z.B., 2013. Removal of uranium(VI) from aqueous solutions by CMK-3 and its polymer composite. Appl. Surf. Sci. 285, 258–266. https://doi.org/10.1016/j.apsusc.2013.08.048.

Manoj, S., Thirumurugan, M., Elango, L., 2020. Determination of distribution coefficient of uranium from physical and chemical properties of soil. Chemosphere 244, 125411. https://doi.org/10.1016/j.chemosphere.2019.125411.

Missana, T., García-Gutiérrez, M., Alonso, Ú., 2004. Kinetics and irreversibility of cesium and uranium sorption onto bentonite colloids in a deep granitic environment. Appl. Clay Sci. 26, 137–150. https://doi.org/10.1016/j.clay.2003.09.008.

Niu, Z.W., Fan, Q.H., Wang, W.H., Xu, J.Z., Chen, L., Wu, W.S., 2009. Effect of pH, ionic strength and humic acid on the sorption of uranium(VI) to attapulgite. Appl. Radiat. Isot. 67, 1582–1590. https://doi.org/10.1016/j.apradiso.2009.03.113.

Niu, Z.W., Wei, X.Y., Qiang, S.R., Wu, H.Y., Pan, D.Q., Wu, W.S., Fan, Q.H., 2019. Spectroscopic studies on U(VI) incorporation into $CaCO_3$: effects of aging time and U (VI) concentration. Chemosphere 220, 1100–1107. https://doi.org/10.1016/j.chemosphere.2019.01.010.

Richter, C., Müller, K., Drobot, B., Steudtner, R., Großmann, K., Stockmann, M., Brendler, V., 2016. Macroscopic and spectroscopic characterization of uranium(VI) sorption onto orthoclase and muscovite and the influence of competing Ca^{2+}. Geochem. Cosmochim. Acta 189, 143–157. https://doi.org/10.1016/j.gca.2016.05.045.

Roberts, H.E., Morris, K., Law, G.T.W., Mosselmans, J.F.W., Bots, P., Kvashnina, K., Shaw, S., 2017. Uranium(V) incorporation mechanisms and stability in Fe(II)/Fe(III) (oxyhydr)oxides. Environ. Sci. Technol. Lett. 4, 421–426. https://doi.org/10.1021/acs.estlett.7b00348.

Rout, S., Ravi, P.M., Kumar, A., Tripathi, R.M., 2015. Study on speciation and salinity-induced mobility of uranium from soil. Environ. Earth Sci. 74, 2273–2281. https://doi.org/10.1007/s12665-015-4218-9.

Sachs, S., Bernhard, G., 2008. Sorption of U(VI) onto an artificial humic substance-kaolinite-associate. Chemosphere 72, 1441–1447. https://doi.org/10.1016/j.chemosphere.2008.05.027.

Sani, R.K., Peyton, B.M., Amonette, J.E., Geesey, G.G., 2004. Reduction of uranium(VI) under sulfate-reducing conditions in the presence of Fe(III)-(hydr)oxides. Geochem. Cosmochim. Acta 68, 2639–2648. https://doi.org/10.1016/j.gca.2004.01.005.

Sharma, P., Tomar, R., 2011. Sorption behaviour of nanocrystalline MOR type zeolite for Th(IV) and Eu(III) removal from aqueous waste by batch treatment. J. Colloid Interface Sci. 362, 144–156. https://doi.org/10.1016/j.jcis.2011.06.030.

Sheng, G., Hu, J., Alsaedi, A., Shammakh, W., Monaquel, S., Ye, F., Li, H., Huang, Y., Alshomrani, A.S., Hayat, T., Ahmad, B., 2015. Interaction of uranium(VI) with titanate nanotubes by macroscopic and spectroscopic investigation. J. Mol. Liq. 212, 563–568. https://doi.org/10.1016/j.molliq.2015.10.018.

Shi, Y.L., He, J., Yang, X., Zhou, W., Wang, J., Li, X., Liu, C.L., 2019. Sorption of U(VI) onto natural soils and different mineral compositions: the batch method and spectroscopy analysis. J. Environ. Radioact. 203, 163–171. https://doi.org/10.1016/j.jenvrad.2019.03.011.

Sihn, Y., Yun, J. I.l, Lee, W., 2016. Laser spectroscopic characterization and quantification of uranium(VI) under fluorescence quenching by Fe(II). J. Radioanal. Nucl. Chem. 308, 413–423. https://doi.org/10.1007/s10967-015-4428-3.

Soliman, N.K., Moustafa, A.F., 2020. Industrial solid waste for heavy metals adsorption features and challenges; a review. J. Mater. Res. Technol. 9, 10235–10253. https://doi.org/10.1016/j.jmrt.2020.07.045.

Tan, L.Q., Tan, X.L., Ren, X.M., Mei, H.Y., Wang, X.K., 2018. Influence of pH, soil humic acid, ionic strength and temperature on sorption of U(VI) onto attapulgite. J. Radioanal. Nucl. Chem. 316, 981–991. https://doi.org/10.1007/s10967-018-5795-3.

Ten Hulscher, T.E.M., Cornelissen, G., 1996. Effect of temperature on sorption equilibrium and sorption kinetics of organic micropollutants - a review. Chemosphere 32, 609–626. https://doi.org/10.1016/0045-6535(95)00345-2.

Tertre, E., Berger, G., Simoni, E., Castet, S., Giffaut, E., Loubet, M., Catalette, H., 2006. Europium retention onto clay minerals from 25 to 150 °C: experimental measurements, spectroscopic features and sorption modelling. Geochem. Cosmochim. Acta 70, 4563–4578. https://doi.org/10.1016/j.gca.2006.06.1568.

Tournassat, C., Tinnacher, R.M., Grangeon, S., Davis, J.A., 2018. Modeling uranium(VI) adsorption onto montmorillonite under varying carbonate concentrations: a surface complexation model accounting for the spillover effect on surface potential. Geochem. Cosmochim. Acta 220, 291–308. https://doi.org/10.1016/j.gca.2017.09.049.

Troyer, L.D., Maillot, F., Wang, Zheming, Wang, Zimeng, Mehta, V.S., Giammar, D.E., Catalano, J.G., 2016. Effect of phosphate on U(VI) sorption to montmorillonite: ternary complexation and precipitation barriers. Geochem. Cosmochim. Acta 175, 86–99. https://doi.org/10.1016/j.gca.2015.11.029.

Uddin, M.K., 2017. A review on the adsorption of heavy metals by clay minerals, with special focus on the past decade. Chem. Eng. J. 308, 438–462. https://doi.org/10.1016/j.cej.2016.09.029.

Van Der Weijden, R.D., Meima, J., Comans, R.N.J., 1997. Sorption and sorption reversibility of cadmium on calcite in the presence of phosphate and sulfate. Mar. Chem. 57, 119–132. https://doi.org/10.1016/S0304-4203(97)00018-2.

Vijaya, Y., Popuri, S.R., Boddu, V.M., Krishnaiah, A., 2008. Modified chitosan and calcium alginate biopolymer sorbents for removal of nickel(II) through adsorption. Carbohydr. Polym. 72, 261–271. https://doi.org/10.1016/j.carbpol.2007.08.010.

Wang, J.J., He, B.H., Wei, X.Y., Li, P., Liang, J.J., Qiang, S.R., Fan, Q.H., Wu, W.S., 2019. Sorption of uranyl ions on TiO_2: effects of pH, contact time, ionic strength, temperature and HA. J. Environ. Sci. 75, 115–123. https://doi.org/10.1016/j.jes.2018.03.010.

Wang, J.J., Wang, Y., Wang, W., Ding, Z., Geng, R.Y., Li, P., Pan, D.Q., Liang, J.J., Qin, H. B., Fan, Q.H., 2020. Tunable mesoporous g-C_3N_4 nanosheets as a metal-free catalyst for enhanced visible-light-driven photocatalytic reduction of U(VI). Chem. Eng. J. 383, 123193. https://doi.org/10.1016/j.cej.2019.123193.

Wang, J.L., Guo, X., 2020. Adsorption kinetic models: physical meanings, applications, and solving methods. J. Hazard Mater. 390, 122156. https://doi.org/10.1016/j.jhazmat.2020.122156.

Wang, S., Boyjoo, Y., Choueib, A., Zhu, Z.H., 2005. Removal of dyes from aqueous solution using fly ash and red mud. Water Res. 39, 129–138. https://doi.org/10.1016/j.watres.2004.09.011.

Wu, D.B., Zhao, J., Zhang, L., Wu, Q.S., Yang, Y.H., 2010. Lanthanum adsorption using iron oxide loaded calcium alginate beads. Hydrometallurgy 101, 76–83. https://doi.org/10.1016/j.hydromet.2009.12.002.

Xie, Y., Chen, C.L., Ren, X.M., Wang, X.X., Wang, H.Y., Wang, X.K., 2019. Emerging natural and tailored materials for uranium-contaminated water treatment and environmental remediation. Prog. Mater. Sci. 103, 180–234. https://doi.org/10.1016/j.pmatsci.2019.01.005.

Xu, D., Tan, X.L., Chen, C.L., Wang, X.K., 2008. Adsorption of Pb(II) from aqueous solution to MX-80 bentonite: effect of pH, ionic strength, foreign ions and temperature. Appl. Clay Sci. 41, 37–46. https://doi.org/10.1016/j.clay.2007.09.004.

Yan, Y., Chen, C.C., 2010. Thermodynamic modeling of CO_2 solubility in aqueous solutions of NaCl and Na_2SO_4. J. Supercrit. Fluids 55, 623–634. https://doi.org/10.1016/j.supflu.2010.09.039.

Yang, S.T., Zhao, D.L., Zhang, H., Lu, S.S., Chen, L., Yu, X.J., 2010. Impact of environmental conditions on the sorption behavior of Pb(II) in Na-bentonite suspensions. J. Hazard Mater. 183, 632–640. https://doi.org/10.1016/j.jhazmat.2010.07.072.

Yang, X.Y., Ge, X.K., He, J.G., Wang, C.L., Qi, L.Y., Wang, X.Y., Liu, C.L., 2018. Effects of mineral compositions on matrix diffusion and sorption of ^{75}Se(IV) in granite. Environ. Sci. Technol. 52, 1320–1329. https://doi.org/10.1021/acs.est.7b05795.

Zhang, C.L., Li, X., Chen, Z.S., Wen, T., Huang, S.Y., Hayat, T., Alsaedi, A., Wang, X.K., 2018. Synthesis of ordered mesoporous carbonaceous materials and their highly efficient capture of uranium from solutions. Sci. China Chem. 61, 281–293. https://doi.org/10.1007/s11426-017-9132-7.

Zhang, H.X., Zhao, X., Wei, J.Y., Li, F.Z., 2015. Removal of cesium from low-level radioactive wastewaters using magnetic potassium titanium hexacyanoferrate. Chem. Eng. J. 275, 262–270. https://doi.org/10.1016/j.cej.2015.04.052.

Zhang, Y.Y., Lv, J.W., Dong, X.J., Fang, Q., Tan, W.F., Wu, X.Y., Deng, Q.W., 2020. Influence on uranium(VI) migration in soil by iron and manganese salts of humic acid: mechanism and behavior. Environ. Pollut. 256, 113369. https://doi.org/10.1016/j.envpol.2019.113369.

Zhao, D.L., Wang, X.B., Yang, S.T., Guo, Z.Q., Sheng, G.D., 2012. Impact of water quality parameters on the sorption of U(VI) onto hematite. J. Environ. Radioact. 103, 20–29. https://doi.org/10.1016/j.jenvrad.2011.08.010.

Zhou, W.Q., Xian, D.F., Su, X.B., Li, Y., Que, W.M., Shi, Y.L., Wang, J.Y., Liu, C.L., 2020. Macroscopic and spectroscopic characterization of U(VI) sorption on biotite. Chemosphere 255, 126942. https://doi.org/10.1016/j.chemosphere.2020.126942.